
Model-X Change-Point Detection of Conditional Distribution

Yiwen Huang*

Department of Statistics
Peking University
2401210080@stu.pku.edu.cn

Yan Dong*

International Institute of Finance, School of Management
University of Science and Technology of China
apriloa@mail.ustc.edu.cn

Mengying Yan

Department of Biostatistics & Bioinformatics
Duke University School of Medicine
mengying.yan@duke.edu

Ziye Tian

Department of Biostatistics & Bioinformatics
Duke University School of Medicine
ziye.tian@duke.edu

Chuan Hong

Department of Biostatistics & Bioinformatics
Duke University School of Medicine
chuan.hong@duke.edu

Doudou Zhou[†]

Department of Statistics and Data Science
National University of Singapore
ddzhou@nus.edu.sg

Molei Liu[†]

Department of Biostatistics, Peking University Health Science Center
Beijing International Center for Mathematical Research, Peking University
moleiliu@bjmu.edu.cn

Abstract

The dynamic nature of many real-world systems can lead to temporal outcome model shifts, causing a deterioration in model accuracy and reliability over time. This requires change-point detection on the outcome models to guide model re-training and adjustments. However, inferring the change point of conditional models is more prone to loss of validity or power than classic detection problems for marginal distributions. This is due to both the temporal covariate shift and the complexity of the outcome model. To address these challenges, we propose a novel model-X Conditional Random Testing (CRT) method computationally enhanced with latent mixture model (LMM) distillation for simultaneous change-point detection and localization of the conditional outcome model. Built upon the model-X framework, our approach can effectively adjust for the potential bias caused by the temporal covariate shift and allow the flexible use of general machine learning methods for outcome modeling. It preserves good validity against complex or erroneous outcome models, even with imperfect knowledge of the temporal covariate shift learned from some auxiliary unlabeled data. Moreover, the incorporation of LMM distillation significantly reduces the computational burden of the CRT by eliminating the need for repeated complex model refitting in its resampling procedure and preserves the statistical validity and power well. Theoretical validity of the proposed method is justified. Extensive simulation studies and a real-world example demonstrate the statistical effectiveness and computational scalability of our method as well as its significant improvements over existing methods.

*Equal Contribution

[†]Corresponding author. To whom correspondence should be addressed.

1 Introduction

1.1 Background

The advancement of experimental technologies has made large-scale data featuring high-dimensional covariates readily available. Modern developed machine learning techniques have leveraged such big data to develop prediction models for uncovering underlying patterns and facilitating data-driven decision-making. However, due to the dynamic nature of many real-world systems, model performances may shift over time, leading to inaccuracies in models (Davis et al., 2020). For example, a case study on Acute Kidney Injury (AKI) found that seven parallel machine learning models, trained using data from 2003, showed deteriorating model performance when evaluated over the next nine years in a validation cohort (Davis et al., 2017). Therefore, it becomes necessary to develop a change point detection method for detecting shifts in model performance, which could indicate that the current model is no longer effective.

In recent years, there has been a growing literature on the change point detection methods for identifying the possible changes in the distribution properties of temporal data sequences. However, most existing change point detection methods predominantly focus on identifying changes in the marginal distribution of the observations. These methods are not applicable for predictive modeling tasks, of which the primary interest lies in understanding whether and when the relationship between a response and covariates. For example, changes in the conditional distribution of health outcomes given clinical indicators (Gao et al., 2025), or stock returns conditional on market factors (Vogt (2015)), may significantly affect the reliability of predictive models over time. Similar issues are also encountered in environmental analysis (Cai et al., 2000), power systems (Chen et al., 2016), and meteorology (Harris et al., 2022).

Furthermore, due to the sensitive nature of the data or the high cost of manual labeling, the availability of labeled data remains scarce, which is a common issue in domains such as electronic health records (Humbert-Droz et al., 2022), financial transactions (Kennedy et al., 2024), and social networks (Li et al., 2022). The scarcity of the labeled data and the high dimensionality may pose additional challenges for detecting change points in conditional distributions. Therefore, our goal is to develop a method for detecting and localizing change points in conditional distributions under high-dimensional settings with limited labeled data.

1.2 Problem setup

Suppose that we have T time points and at each time point $t \in \{1, \dots, T\}$, we observe a dataset $\mathcal{D}_t = \{(Y_i^{[t]}, \mathbf{X}_i^{[t]})\}_{i=1}^{n_t}$, where $Y_i^{[t]} \in \mathbb{R}$ represents the outcome of interest, $\mathbf{X}_i^{[t]} \in \mathbb{R}^p$ denotes a vector of features possibly with high-dimensionality or complex effects on $Y_i^{[t]}$, and n_t is the number of observations at t . By concatenating all the samples across time points, we can write the full set of observations as: $\mathcal{D} = \{(Y_i, \mathbf{X}_i, R_i)\}_{i=1}^n$, where $n = \sum_{t=1}^T n_t$ is the total sample size and $R_i \in \{1, \dots, T\}$ serves as the time label indicating the time point associated with each observation. Since the temporal information is now fully captured by the time labels R_i , the superscripts $[t]$ on Y_i and \mathbf{X}_i are omitted for notational simplicity. For the assignment of time labels R_i , it can be illustrated as follows

$$R_1 = \dots = R_{n_1} = 1, \quad \underbrace{R_{n_1+1} = \dots = R_{n_1+n_2}}_{n_2} = 2, \quad \dots, \quad \underbrace{R_{n_1+\dots+n_{T-1}+1} = \dots = R_n}_{n_T} = T.$$

Specifically, the first n_1 observations are associated with $R_i = 1$, the next n_2 observations are associated with $R_i = 2$, and so forth, until the last n_T observations, which are associated with $R_i = T$. Denote $N_\tau = \sum_{t=1}^\tau n_t$.

Given R_i , each observation (Y_i, \mathbf{X}_i) is assumed to follow the generative model: $Y, \mathbf{X} \mid R \sim p_{\mathbf{X}|R}(\mathbf{X})p_{Y|\mathbf{X}, R}(Y)$, where $p_{\mathbf{X}|R}$, the marginal distribution of \mathbf{X} , is allowed to vary across time points R . Our objective is to test whether the conditional distribution of $Y \mid \mathbf{X}, R$ remains invariant over time. Specifically, we aim to test the null hypothesis:

$$H_0 : p_{Y|\mathbf{X}, R}(y) = p_{Y|\mathbf{X}}(y), \quad R = 1, \dots, T \quad (1)$$

against the change-point alternative

$$H_1 : \quad \exists 1 \leq \tau < T, \quad \text{s.t.} \quad p_{Y|\mathbf{X}, R}(y) = \begin{cases} p_{Y|\mathbf{X}}(y), & R \leq \tau, \\ q_{Y|\mathbf{X}}(y), & \text{otherwise,} \end{cases} \quad (2)$$

where $p_{Y|\mathbf{X}} \neq q_{Y|\mathbf{X}}$.

To detect changes in the conditional distribution $Y | \mathbf{X}, R$, our work builds upon the model-X conditional random testing (CRT) (Candès et al., 2018) framework, which assumes that the conditional distribution $p(R | \mathbf{X})$ is known or well-approximated. Since $p(R | \mathbf{X})$ is typically unknown in practice, we can leverage an abundant set of unlabeled samples $\{(\mathbf{X}_i, R_i)\}_{i=n+1}^N$, which provide valuable information about the relationship between covariates and time, thereby improving the estimation of $p(R | \mathbf{X})$ and further enhancing the validity of our proposed method.

1.3 Related literature

Existing change point methods for paired data (\mathbf{X}, Y) mainly detect the changes in the conditional expectation of Y given \mathbf{X} . Early studies assume a linear model and examine the changes in the slope (Kim and Siegmund, 1989; Kim and Cai, 1993; Andrews et al., 1996; Bai, 1997; Julius, 2001; Gombay, 2010). This line of work has been extended to high-dimensional settings, seasonality, and dependence structures (Robbins et al., 2016; Lee et al., 2016; Rinaldo et al., 2021; Wang et al., 2021). However, their parametric assumption and linear limitation may fail to capture the changes in nonlinear or complex models.

To address these limitations, nonparametric approaches have been proposed. Early works, such as Müller (1992) and Loader (1996), focused on locating changes using nonparametric regression, under the assumption of fixed, univariate, and equally spaced covariates. Other studies (Su and Xiao, 2008; Su and White, 2010; Vogt, 2015) tested the stability of the conditional mean function but did not address the localization of change points.

More recently, Nie and Nicolae (2022) introduced a kernel-based approach for detecting and localizing changes in the conditional distribution under random design. Despite its effectiveness in modeling complex relationship, the kernel-based method, along with its asymptotic properties, indicates that it is not applicable for high-dimensional settings. Moreover, all the aforementioned methods assume only one observation per time point and the diverging time horizon T , which differs from our setting with multiple observations per time point and fixed T .

In high-dimensional complex models with limited data, an effective method for testing the conditional independence is the model-X conditional random testing (CRT) (Candès et al., 2018). It has gained increasing popularity for its ability to control the Type-I error rate non-asymptotically, regardless of the test statistic or assumptions about the conditional distribution of the response given covariates. However, the high computational burden in the resample steps has been a critical limitation.

Recent advancements in CRT have focused on enhancing computational efficiency (Bates et al., 2020; Tansey et al., 2022; Liu et al., 2022). In particular, Liu et al. (2022) proposed the distilled CRT (dCRT), which substantially reduces computational costs while maintaining high statistical power and exact validity. Despite their effectiveness, these methods are not directly applicable to change-point detection. Change points require fitting separate models over time, complicating the construction of test statistics and invalidating the original distillation techniques. A key challenge remains: how to simplify high-dimensional models into low-dimensional forms during the repeated refitting of CRTs, in order to reduce computational burden while retaining validity.

1.4 Our contribution

In this paper, we propose the Model-X changE-point detectioN of conditional Distribution (MEND) algorithm. MEND utilizes the CRT method with latent mixture model (LMM) distillation to enable the simultaneous detection and localization of change points in the conditional distribution of a response given high-dimensional covariates. The major contributions of this paper are threefold. First, we tailor a model-X based CRT method for the proposed change-point detection problem, which leverages both labeled and unlabeled data to fully extract informative patterns from the data. Moreover, inheriting the attractive properties of the model-X framework, our proposed method does not require any specific assumptions on the conditional distribution of responses given covariates.

Second, to reduce the computational burden of the proposed CRT procedure, we introduce a **LA**tent mixture model **D**istillation procedure, named MEND-LAD. By accurately pre-training the global model as a latent mixture model (LMM), we replace the repeated high-dimensional fittings in MEND with simple low-dimensional regression, which significantly reduces the computational burden while maintaining statistical validity. Importantly, this LAD strategy differs substantially from dCRT (Liu et al., 2022) in that our method effectively leverages the LMM structure under the alternative hypothesis of the change point problem to extract models or representations not captured by dCRT but informative for inference of the change point.

Finally, we provide theoretical analysis showing that both MEND and MEND-LAD achieve valid Type-I error control in the asymptotic sense under the null hypothesis of no distributional change. Extensive numerical experiments evidence the effectiveness of the proposed methods.

2 Method

The null hypothesis H_0 asserts that the distribution of Y given \mathbf{X} and R is identical to the distribution of Y given \mathbf{X} alone, for all time points. In other words, Y is conditionally independent of R given \mathbf{X} , denoted as $Y \perp\!\!\!\perp R | \mathbf{X}$. Framing the problem as a conditional independence test allows us to apply a Conditional Randomization Test (CRT) to detect change points effectively.

2.1 Conditional Randomization Testing (CRT)

The CRT, introduced by Candès et al. (2018), is a framework for conditional independence testing that provides exact (non-asymptotic) control of Type-I error with the perfect knowledge of the conditional distribution of $R | \mathbf{X}_i$. It operates within the model-X framework, which assumes the distribution of $R | \mathbf{X}_i$ is known or can be estimated, rather than making assumptions about $Y | \mathbf{X}, R$. CRT relies on a user-defined test statistic S . The choice of S is completely flexible, and the validity of the CRT remains intact. CRT generates counterfactual datasets by resampling R_i while preserving the conditional structure of $R_i | \mathbf{X}_i$. For each resampled dataset, the test statistic S is recomputed, and the p -value is obtained by ranking the observed test statistic among the resampled values. The procedure is summarized in Algorithm 1, with its strict validity established in Theorem 2.1.

Algorithm 1 Conditional Randomization Test (CRT) Framework

- 1: **Input:** A set of n independent samples $\mathcal{D} = \{(Y_i, \mathbf{X}_i, R_i)\}_{1 \leq i \leq n}$. Test statistic $S(\mathcal{D})$, number of randomization K , and nominal significance level $\alpha \in (0, 1)$.
- 2: **Output:** A p -value for testing H_0 against H_1 defined in (1) and (2).
- 3: **Randomization:**
- 4: **for** $k = 1, 2, \dots, K$ & $i = 1, \dots, n$ **do**
- 5: Randomly generate $R_i^{(k)}$ from $p_{R|\mathbf{X}_i}(t)$ independently from (Y_i, R_i) , while keeping \mathbf{X}_i and Y_i unchanged, resulting in the resampled data set $\mathcal{D}^{(k)} = \{(Y_i, \mathbf{X}_i, R_i^{(k)})\}_{1 \leq i \leq n}$.
- 6: **end for**
- 7: **Compute p -value:**

$$p\text{-value} = \frac{1}{K+1} \left(1 + \sum_{k=1}^K \mathbb{I}(S(\mathcal{D}^{(k)}) \geq S(\mathcal{D})) \right),$$

where $\mathbb{I}(\cdot)$ is the indicator function. Reject H_0 if $p\text{-value} \leq \alpha$.

Theorem 2.1 (Strict validity of CRT). *When $H_0 : p_{Y|\mathbf{X}, R}(y) = p_{Y|\mathbf{X}}(y)$ holds for $R = 1, \dots, T$,*

$$\lim_{n \rightarrow \infty} \mathbb{P}(\text{Algorithm 1 rejects}) \leq \alpha.$$

2.2 Model-X Change-Point Detection (MEND)

The MEND method builds upon the CRT framework described above. For each potential change point τ , MEND estimates some models (e.g. conditional expectation) of Y given \mathbf{X} separately on the samples before and after τ , denoted by $\hat{f}_-^\tau(Y | \mathbf{X})$ and $\hat{f}_+^\tau(Y | \mathbf{X})$, respectively. The divergence

between these models is computed to identify the most likely change point. While the specific form of \hat{f} depends on the modeling approach, the framework is flexible and allows \hat{f} to be derived from a wide range of predictive models, including parametric methods and complex machine learning.

In general, for each potential change point $\tau \in \{1, \dots, T-1\}$, the conditional models $\hat{f}_-^\tau(Y | \mathbf{X})$ and $\hat{f}_+^\tau(Y | \mathbf{X})$ can be estimated by solving the following optimization problem:

$$\begin{aligned}\hat{f}_-^\tau(Y | \mathbf{X}) &= \arg \min_{\theta} \mathcal{L}_-(\theta; \{Y_i, \mathbf{X}_i\}_{i=1}^{n_-^\tau}), \\ \hat{f}_+^\tau(Y | \mathbf{X}) &= \arg \min_{\theta} \mathcal{L}_+(\theta; \{Y_i, \mathbf{X}_i\}_{i=n_-^\tau+1}^n),\end{aligned}\tag{3}$$

where $\mathcal{L}_-(\theta; \cdot)$ and $\mathcal{L}_+(\theta; \cdot)$ are loss functions tailored to the specific model \hat{f} , θ denotes the model parameters, and $n_-^\tau = \sum_{i=1}^\tau n_i$.

The test statistic S is computed by evaluating the divergence between $\hat{f}_-^\tau(Y | \mathbf{X})$ and $\hat{f}_+^\tau(Y | \mathbf{X})$ across all potential change points τ :

$$S(\mathcal{D}) = \max_{\tau \in \{1, \dots, T-1\}} \text{dvg}(\hat{f}_-^\tau(Y | \mathbf{X}), \hat{f}_+^\tau(Y | \mathbf{X})),\tag{4}$$

where $\text{dvg}(\cdot, \cdot)$ measures the divergence between the two models, indicating the likelihood of a change point at τ . For example, $\text{dvg}(\cdot, \cdot)$ could be defined as the mean squared difference:

$$\text{dvg}(\hat{f}_-^\tau, \hat{f}_+^\tau) = \frac{1}{n} \sum_{i=1}^n \left(\hat{f}_-^\tau(\mathbf{X}_i) - \hat{f}_+^\tau(\mathbf{X}_i) \right)^2.\tag{5}$$

2.3 Distilled Change-Point Detection (MEND-LAD)

The original MEND procedure is computationally intensive due to the repeated computation of \hat{f}_-^τ and \hat{f}_+^τ when constructing the test statistic S with all K counterfeit datasets $\mathcal{D}^{(k)}$, as outlined in Algorithm 1. This cost becomes especially prohibitive when \mathbf{X} is high-dimensional and complicated machine learning methods (e.g., neural networks) are employed to learn $Y | \mathbf{X}, R$.

To address this, we introduce MEND-LAD, a faster alternative based on Latent mixture model Distillation (LAD) that could still maintain close statistical performance to MEND. The core idea is to learn a distilled, low-dimensional representation $d(\mathbf{X})$ capturing the predictive information in $Y \sim \mathbf{X}, R$ without using the observed R . Here, it is crucial to “mask” R when learning $d(\mathbf{X})$ because it helps to avoid refitting the high-dimensional or complex learning algorithms with the resampled $R^{(k)}$ in Algorithm 1. In specific, we can reduce the cost of computing the test statistic $S(\{Y, \mathbf{X}, t\})$ to $S(\{Y, d(\mathbf{X}), t\})$ with much lower-dimensional predictors $d(\mathbf{X})$, while maintaining the exact validity because $S(\{Y, d(\mathbf{X}), t\})$ can be viewed as a special case of $S(\{Y, \mathbf{X}, t\})$ and Theorem 2.1 is still applicable.

Remark 2.2. A conceptually similar idea of distillation has been adopted in dCRT (Liu et al., 2022). However, our LAD procedure to be introduced next is essentially different from dCRT in that we can effectively leverage the LMM structure in the change-point regime to distill more informative representations than dCRT.

Under the alternative hypothesis H_1 , the distribution of $Y | \mathbf{X}$ changes at some underlying time point τ , leading to a distributional shift between $Y | \mathbf{X}, R \leq \tau$ and $Y | \mathbf{X}, R > \tau$. To model $Y | \mathbf{X}$ without conditioning on R , we consider a latent mixture model (LMM) framework. In this LMM, we introduce a latent binary Z as an indicator for the unobserved status: $Z_i = \mathbb{I}\{R_i > \tau\}$, where $Z_i = 0$ indicates the pre-change regime and $Z_i = 1$ the post-change. Conditional on Z , we model $Y \sim X$ using: $p(Y | \mathbf{X}, Z = z) = p_z(Y | \mathbf{X})$ for $z \in \{0, 1\}$. The logarithmic likelihood for $Y \sim X$ (without Z) is then written as:

$$\log p(Y, \mathbf{X}) = \sum_{i=1}^n \log [\pi_0(\mathbf{X}_i)p_0(Y_i | \mathbf{X}_i) + (1 - \pi_0(\mathbf{X}_i))p_1(Y_i | \mathbf{X}_i)]$$

where $\pi_0(\mathbf{X})$ and $1 - \pi_0(\mathbf{X})$ are the prior probability weights for the regimes before and after the change point, respectively. Based on this, we can extract the representation $d(\mathbf{X})$ informative to $p_0(Y | \mathbf{X})$, $p_1(Y | \mathbf{X})$ by maximizing $\log p(Y, \mathbf{X})$ with respect to the unknown models

$\{\pi_0, \pi_1, p_0, p_1\}$. This could be realized under certain model specification using the Expectation-Maximization algorithm introduced in Appendix A.

MEND-LAD (mean): Conditional Mean-Based Distillation. The simplest form of distillation, denoted as $d_0(\mathbf{X})$, uses only the conditional means estimated by the EM algorithm. Specifically, the EM algorithm outputs $\hat{m}_0(\mathbf{X})$ and $\hat{m}_1(\mathbf{X})$, which approximate the conditional means of Y in the pre-change and post-change regimes, respectively. The distilled representation $d_0(\mathbf{X})$ is constructed as: $d_0(\mathbf{X}) = \{\hat{m}_0(\mathbf{X}), \hat{m}_1(\mathbf{X})\}$.

For each candidate change point τ , MEND-LAD splits the data into subsets $R \leq \tau$ and $R > \tau$, and computes the test statistic using the model: $Y_i \sim a\hat{m}_0(\mathbf{X}_i) + (1-a)\hat{m}_1(\mathbf{X}_i)$, where the mixing coefficients $\hat{a}_{\tau-}$ and $\hat{a}_{\tau+}$ for the pre- and post-change regimes are computed as follows:

$$\begin{aligned}\hat{a}_{\tau-} &= \arg \min_a \sum_{i=1}^{n_-} (Y_i - a\hat{m}_0(\mathbf{X}_i) - (1-a)\hat{m}_1(\mathbf{X}_i))^2 + \lambda(a - 0.5)^2, \\ \hat{a}_{\tau+} &= \arg \min_a \sum_{i=n_-}^T (Y_i - a\hat{m}_0(\mathbf{X}_i) - (1-a)\hat{m}_1(\mathbf{X}_i))^2 + \lambda(a - 0.5)^2,\end{aligned}\tag{6}$$

where λ is a small regularizing parameter to avoid singularity issues. The divergence between the two subsets is measured using the estimated mixing coefficients $\hat{a}_{\tau-}$ and $\hat{a}_{\tau+}$, and the test statistic is defined as: $S(\mathcal{D}) = \max_{\tau \in \{1, \dots, T-1\}} |\hat{a}_{\tau-} - \hat{a}_{\tau+}|$. The d_0 approach focuses solely on the conditional means, making it computationally efficient and suitable for scenarios where the conditional mean captures the essential information about the relationship between Y and \mathbf{X} .

MEND-LAD (repr): representation Based Distillation. We define $d_1(\mathbf{X})$ as a low-dimensional representation of \mathbf{X} that retains essential information for modeling $Y \mid \mathbf{X}$. This construction generalizes $d_0(\mathbf{X})$, which consists solely of predictive means $(\hat{m}_0(\mathbf{X}), \hat{m}_1(\mathbf{X}))$. It could provide robustness against model mis-specification, and preserve effectiveness when there are multiple change points under H_1 , where the two-mixture model may be insufficient. In practice, the form of $d_1(\mathbf{X})$ can vary depending on the modeling strategy. For example, it could be the penultimate layer of a neural network trained to predict $Y \mid \mathbf{X}$, or an augmentation of $d_0(\mathbf{X})$ with the most influential input characteristics identified using the EM algorithm. Specifically, let B_0 and B_1 denote the sets of indices corresponding to the top k features (e.g., based on coefficient magnitude) from the fitted models \hat{m}_0 and \hat{m}_1 , respectively. Then, we define $d_1(\mathbf{X}) = \{\hat{m}_0(\mathbf{X}), \hat{m}_1(\mathbf{X}), \mathbf{X}_{:B_0 \cup B_1}\}$. Our framework is designed to be flexible and can incorporate any such representation that facilitates sensitive and robust inference.

2.4 Learning $R \mid \mathbf{X}$

Our methods require knowledge of the conditional distribution $p(R \mid \mathbf{X})$ under the model-X framework. This distribution is typically unknown in practical and could be estimated using classification methods for $R \sim \mathbf{X}$. In general, logistic regression or modern machine learning methods can be employed for this purpose. In the semi-supervised setting, we could leverage an abundant set of unlabeled samples $\{(\mathbf{X}_i, R_i)\}_{i=n+1}^N$ to learn $p(R \mid \mathbf{X})$. This will allow for a more accurate estimate of $p(R \mid \mathbf{X})$, thus improving the validity and power of the CRT procedure. All of our simulation and real-world studies are conducted in this semi-supervised scenario.

3 Numerical Simulation

3.1 Simulation Setup

We consider a semi-supervised setting where we have a small number of labeled data of $\{(Y_i, \mathbf{X}_i, R_i)\}_{i=1}^n$ for testing and large unlabeled data $\{(\mathbf{X}_i, R_i)\}_{i=n+1}^N$ for modeling $R \mid \mathbf{X}$. Specifically, we consider a total of $T = 10$ time points and set the change point position at $\tau = 7$. At each time point t , $n_t = 100$ labeled observations are generated, with a total labeled sample size of $n = \sum_{t=1}^{10} n_t = 1000$. For each observation, the covariate vector $\mathbf{X}_i = (x_{i1}, x_{i2}, \dots, x_{ip})^\top \in \mathbb{R}^p$ consists of both effective and ineffective variables in the outcome model for Y . Unless otherwise

specified, the effective variables are independently sampled from a multivariate normal distribution $N(f(R_i), \Sigma)$, where the time-varying mean function $f(R_i) = 0.2R_i \mathbf{1}_p$ and the covariance matrix $\Sigma = (\Sigma_{k,j})$ with $\Sigma_{k,j} = 0.5^{|k-j|}$. The remaining ineffective variables are independently sampled from the standard normal distribution $N(0, 1)$. Furthermore, for our proposed methods, we consider an unlabeled sample size $N = n + 1000$, unless stated otherwise. For the generation of Y , we consider the following three scenarios, where the first two scenarios are low-dimensional nonlinear models and the third scenario is high-dimensional linear model.

Scenario 1. Set $Y_i = \mathbf{X}_i^\top \boldsymbol{\alpha}^* + \delta_1 x_{i1}^2 + \epsilon_i$, where $\boldsymbol{\alpha}^* = (0.5, -0.5, 0.5, 0.5, 0.5, -0.5, 0, \dots, 0) \in \mathbb{R}^{20}$, and the strength of the nonlinear perturbation δ_1 is varied over $\{0.1, 0.2, 0.3, 0.4, 0.5\}$ to evaluate the ability of each method to control the Type-I error inflation under increasing nonlinear effects. The noise term ϵ_i is independently sampled from $N(0, 1)$, which remains consistent across all scenarios. Furthermore, we conduct an additional experiment by fixing $\delta_1 = 0$ and varying N to assess the quality of model-X in our proposed methods.

Scenario 2. Set $Y_i = \mathbf{S}(\mathbf{X}_i) \boldsymbol{\alpha}^* + \epsilon_i$, if $R_i \leq \tau$, and $Y_i = \mathbf{S}(\mathbf{X}_i)(\boldsymbol{\alpha}^* + \delta_2 \boldsymbol{\beta}) + \epsilon_i$, if $R_i > \tau$, where $\mathbf{X}_i \in \mathbb{R}^5$ is drawn from $N(g(R_i), \Sigma)$ with $g(R_i) = \mathbf{0}$ for $R_i \leq 5$ and $g(R_i) = 0.2R_i \mathbf{1}_5$ otherwise. The transformation $\mathbf{S}(\mathbf{X}_i) = (\sin(x_{i1}), x_{i2}^3, x_{i3}^2, x_{i4}, x_{i5}^2)$ induces nonlinear effects. Here, we set $\boldsymbol{\alpha}^* = (0.5, -0.5, 0.5, 0.5, -0.5)$ and $\boldsymbol{\beta} = (0.05, 0.05, 0.05, 0.05, 0.05)$. The signal strength of structural change δ_2 is set as 0 and 3 to examine the ability to control Type-I error in the presence of covariate shift without structural change, and to assess the power to detect true structural change under a nonlinear model, respectively.

Scenario 3. Set $Y_i = \mathbf{X}_i^\top \boldsymbol{\alpha}^* + \epsilon_i$, if $R_i \leq \tau$, and $Y_i = \mathbf{X}_i^\top (\boldsymbol{\alpha}^* + \delta_3 \boldsymbol{\beta}) + \epsilon_i$, if $R_i > \tau$, where $\boldsymbol{\alpha}^* = (0.5, -0.5, 0.5, 0.5, -0.5, 0, \dots, 0) \in \mathbb{R}^{100}$, $\boldsymbol{\beta} = (0.05, 0.05, 0.05, 0.05, 0.05, 0, \dots, 0) \in \mathbb{R}^{100}$, and the signal strength of the change in the regression coefficients δ_3 is varied over $\{0, 1, 2, 3, 4, 5\}$ to evaluate the power and localization performance under increasing structural change strength in high-dimensional settings.

We compare the proposed methods MEND and MEND-LAD with three benchmark approaches: (1) the ordinary least squares-based CUSUM test (**OLS-CUSUM**) for detecting the changes in low-dimensional parametric models (Ploberger and Krämer, 1992), (2) the dynamic programming method (**DP**) for localizing changes in high-dimensional parametric models (Rinaldo et al., 2021), and (3) the kernel-based methods for detecting changes in conditional expectations and distributions, referred to as **KCE** and **KCD**, respectively (Nie and Nicolae, 2022). To evaluate the performance of the change point detection and localization, we investigate the Type-I error rate and power of testing H_0 against H_1 , the localization accuracy rate, and the run time. The localization accuracy rate is defined as the proportion of replications in which the estimated change point exactly coincides with the true change point. The significance level is set to $\alpha = 0.05$. The implementation details of the methods are provided in Appendix C.

3.2 Simulation Results

Compare MEND and MEND-LAD with existing methods. In Figure 1, we compare the Type-I error control in Scenario 1 and the detection power and localization accuracy in Scenario 3 of our methods with the benchmark methods. Since some methods fail to control the Type-I error rate, we report the power adjusted by subtracting the Type-I error rate in Figure 1(b) to ensure a fair comparison. The Type-I error rate performance for $\delta_3 = 0$ in Scenario 3 is presented in Table 1. Since DP is not designed for change-point testing, we exclude it from Figures 1(a)-1(b) and Table 1. Furthermore, given that OLS-CUSUM is designed for low-dimensional model, we only report the performance of other methods in Scenario 3. As shown in Figures 1 and Table 1, our proposed methods consistently outperform the benchmark methods across all evaluation metrics and scenarios. To be specific, Figure 1(a) demonstrates that the proposed method MEND maintains more stable Type-I error control as the signal strength of the nonlinear term δ_1 increases. In contrast, the Type-I error rate of OLS-CUSUM inflates with the strength of the nonlinear effect, while both KCE and KCD exhibit severe Type-I error inflation, even when the nonlinear effect is small. For instance, when $\delta_1 = 0.3$, the benchmark methods KCD, KCE, and OLS-CUSUM exhibit Type-I error rates of 0.48, 0.4, and 0.1, respectively, while the proposed MEND-LAD (mean) method achieves a much lower rate of 0.046.

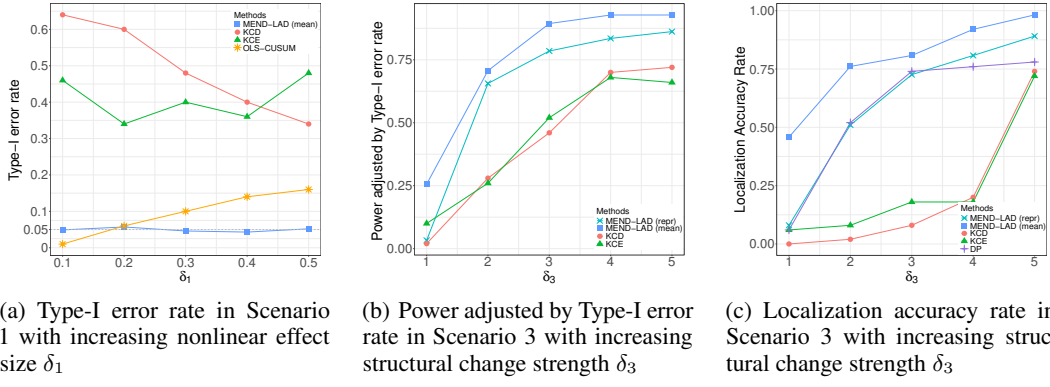


Figure 1: Comparison of Type-I error rate, power and accuracy rate across different scenarios and methods

Table 1: Averaged Type-I error rates of different methods over 500 replications in Scenario 3

δ_3	MEND-LAD (mean)	MEND-LAD (repr)	KCD	KCE
0	0.054	0.057	0.28	0.24

In view of Figures 1(b)-1(c), both the power and the localization accuracy rate of all methods increase as the signal strength of the structural change δ_3 in the regression coefficient grows. However, our proposed methods MEND-LAD (mean) and MEND-LAD (repr) have uniformly higher power and localization accuracy rate than the benchmark methods. For example, when $\delta_3 = 3$, KCD and KCE achieve powers of 0.74 and 0.76 and localization accuracy rates of 0.08 and 0.18, respectively, while MEND-LAD (mean) and MEND-LAD (repr) attain substantially higher powers of 0.959 and 0.842 and localization accuracy rates of 0.808 and 0.726. Similarly, Table 1 shows that the proposed MEND-LAD (mean) and MEND-LAD (repr) methods achieve significantly lower Type-I error rates of 0.054 and 0.057 compared to 0.28 for KCD and 0.24 for KCE, indicating much better error control under the null setting.

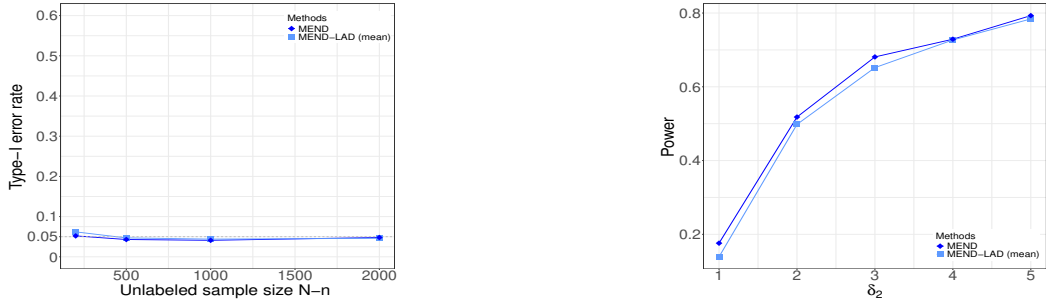
Table 2: Averaged results of different methods over 500 replications in Scenario 2

δ_2	MEND-LAD (mean)	KCD	KCE	DP	OLS-CUSUM	
0	Type-I error rate	0.054	0.63	0.47	-	0.51
3	Power	0.65	0.76	0.39	-	1
	Localization Accuracy Rate	0.65	0.07	0	0.01	0.58

Table 2 compares the Type-I error rate, detection power, and the localization accuracy of different methods in Scenario 2. It shows that our proposed method MEND-LAD (mean) achieves the best overall performance. It maintains the lowest Type-I error rate of 0.054 when the signal strength of structural change $\delta_2 = 0$, while all other methods suffer from severe Type-I error inflation, with rates exceeding 0.45. As δ_2 increases to 3, the proposed method attains a desirable balance between the power and the localization accuracy rate, whereas the benchmarks exhibit either low power or poor localization accuracy.

Compare MEND with MEND-LAD. To comprehensively evaluate the proposed methods MEND and MEND-LAD, we compare their Type-I error control, detection power, and computational efficiency in Figure 2 and Table 3. Specifically, Figure 2(a) shows the Type-I error rates in Scenario 1 with $\delta_1 = 0$ under varying unlabeled sample size $N - n \in \{200, 500, 1000, 2000\}$, while Figure 2(b) illustrates their power performance in Scenario 2 as the structural change strength δ_2 increases. Computational efficiency in the high-dimensional Scenario 3 is summarized in Table 3. Although our proposed methods are implemented in Python and the benchmark methods are implemented in R, the run time remains comparable. In particular, KCD exhibits the highest computational cost, significantly exceeding that of MEND.

Moreover, in view of Figure 2 and Table 3, both MEND-LAD (mean) and MEND-LAD (repr) exhibit a substantial improvement in run time over MEND, benefiting from the designed LLM dis-



(a) Type-I error rate in Scenario 1 with varying unlabeled sample size $N - n$
(b) Power in Scenario 2 with increasing structural change strength δ_2

Figure 2: Comparison of Type-I error control and detection power across the proposed methods

tillation procedure. Meanwhile, MEND and MEND-LAD (mean) exhibit comparable statistical performance in terms of both Type-I error and power. Specifically, both methods effectively control the Type-I error rate below the ideal level 0.05 when the unlabeled sample size $N - n$ exceeds 500. For example, when $N - n = 1000$, MEND and MEND-LAD (mean) achieve Type-I error rates of 0.041 and 0.044, respectively. Furthermore, their detection power improves consistently as the structural change strength δ_2 increases.

Table 3: Averaged run time of different methods over 500 replications in Scenario 3

	MEND	MEND-LAD (mean)	MEND-LAD (repr)	KCD	KCE	DP
Time (seconds)	1154	30	32	4157	211	710

4 Real Data Application

In this section, we apply the developed methods to real-world electronic health records (EHR) data drawn from the Duke University Health System via the Duke Clinical Research Datamart, including all emergency department (ED) visits in 2022. The outcome of interest is a binary variable indicating whether a visit results in inpatient admission to the hospital. The predictors include demographic variables (age, sex, race), vital signs (pulse rate, systolic blood pressure, diastolic blood pressure, oxygen saturation, temperature, respiration rate), and selected comorbidities (local tumor, metastatic tumor, diabetes with complications, diabetes without complications, and renal disease), defined according to ICD codes.

EDs operate in a dynamic clinical environment, and there can be a seasonal model shift in these data—for instance, higher ED visits leading to hospitalization during peak influenza season (Menec et al., 2003). Thus, our goal is to determine whether the proposed MEND algorithm can detect temporal shifts of this nature. We randomly selected a subsample of $n = 1,000$ observations from the full cohort. To avoid possible multiple change points within a single year, we further restricted our analysis to data collected from April through December 2022.

We first conduct a pseudo-simulation based on the covariates in real data and assume that there is no change point. Type-I error for MEND is 0.068 and for MEND-LAD (mean) is 0.045. Type-I error for all the other methods are smaller than 0.05. This indicates a good quality of modeling $R \mid \mathbf{X}$. Details of the pseudo-simulation can be found in Appendix C.2.

We then applied the methods to the original data set. Table 4 shows the estimated change point and corresponding p -values of all methods. Our proposed method MEND and MEND-LAD (mean) give small p -value with estimated change point 11, indicating that there is a change in November. This align with the flu season which potentially lead to the data shift. Baseline DP gives the same point estimation as the proposed method, and other baseline methods have large p -value that not able to identify significant change point. These results illustrate that (i) both versions of our method shows higher statistical power than existing methods; and (ii) our speed-up version MEND-LAD achieves

similar performance (i.e., the same detected change point and close p -values) as MEND requiring refitting complex models with the resampled data sets.

Table 4: Estimated change points and p -values of different methods in our real-world example

	MEND	MEND-LAD (mean)	KCE	KCD	DP	OLS-CUSUM
Estimated τ (month)	11	11	6	8	11	11
p -value	0.016	0.048	0.742	0.6	-	0.55

5 Conclusion

In this paper, we propose the MEND algorithm and its distilled variant MEND-LAD for detecting and localizing the change point in conditional distributions under high-dimensional settings with limited labeled data. MEND constructs an effective test statistic tailored for change-point detection problems within the model-X CRT framework, and leverages both labeled and unlabeled data to enhance testing power and validity. To further alleviate the high computational burden of repeated high-dimensional model fitting in CRT, we design a LMM distillation technique in MEND that replaces high-dimensional refitting with simple low-dimensional regression, significantly improving computational efficiency while preserving statistical validity. Both theoretical properties and numerical studies demonstrate the effectiveness of the proposed method. Future work may extend MEND to multiple change-point scenarios.

References

Andrews, D. W., I. Lee, and W. Ploberger (1996). Optimal changepoint tests for normal linear regression. *Journal of Econometrics* 70(1), 9–38.

Bai, J. (1997). Estimation of a change point in multiple regression models. *Review of Economics and Statistics* 79(4), 551–563.

Bates, S., M. Sesia, C. Sabatti, and E. Candès (2020). Causal inference in genetic trio studies. *Proceedings of the National Academy of Sciences* 117(41), 24117–24126.

Cai, Z., J. Fan, and R. Li (2000). Efficient estimation and inferences for varying-coefficient models. *Journal of the American Statistical Association* 95(451), 888–902.

Candès, E. J., Y. Fan, L. Janson, and J. Lv (2018). Panning for gold: model-x knockoffs for high-dimensional controlled variable selection. *Journal of the Royal Statistical Society: Series B (Statistical Methodology)* 80, 551–577.

Chen, Y. C., T. Banerjee, A. D. Domínguez-García, and V. V. Veeravalli (2016). Quickest line outage detection and identification. *IEEE Transactions on Power Systems* 31(1), 749–758.

Davis, S. E., R. A. Greevy Jr, T. A. Lasko, C. G. Walsh, and M. E. Matheny (2020). Detection of calibration drift in clinical prediction models to inform model updating. *Journal of Biomedical Informatics* 112, 103611.

Davis, S. E., T. A. Lasko, G. Chen, E. D. Siew, and M. E. Matheny (2017). Calibration drift in regression and machine learning models for acute kidney injury. *Journal of the American Medical Informatics Association* 24(6), 1052–1061.

Fan, J. and R. Li (2001). Variable selection via nonconcave penalized likelihood and its oracle properties. *Journal of American Statistical Association* 96, 1348–1360.

Gao, S., R. Addanki, T. Yu, R. A. Rossi, and M. Kocaoglu (2025). Causal discovery-driven change point detection in time series. In *The 28th International Conference on Artificial Intelligence and Statistics*.

Gombay, E. (2010). Change detection in linear regression with time series errors. *Canadian Journal of Statistics* 38(1), 65–79.

Harris, T., B. Li, and J. D. Tucker (2022). Scalable multiple changepoint detection for functional data sequences. *Environmetrics* 33(2), e2710.

Humbert-Droz, M., P. Mukherjee, and O. Gevaert (2022). Strategies to address the lack of labeled data for supervised machine learning training with electronic health records: Case study for the extraction of symptoms from clinical notes. *JMIR Medical Informatics* 10(3), e32903.

Julious, S. A. (2001). Inference and estimation in a changepoint regression problem. *Journal of the Royal Statistical Society: Series D (The Statistician)* 50(1), 51–61.

Kennedy, R. K. L., F. Villanustre, T. M. Khoshgoftaar, and Z. Salekshahrezaee (2024). Synthesizing class labels for highly imbalanced credit card fraud detection data. *Journal of Big Data* 11, 38.

Kim, H.-J. and L. Cai (1993). Robustness of the likelihood ratio test for a change in simple linear regression. *Journal of the American Statistical Association* 88(423), 864–871.

Kim, H.-J. and D. Siegmund (1989). The likelihood ratio test for a change-point in simple linear regression. *Biometrika* 76(3), 409–423.

Lee, S., M. H. Seo, and Y. Shin (2016). The lasso for high dimensional regression with a possible change point. *Journal of the Royal Statistical Society: Series B (Statistical Methodology)* 78(1), 193–210.

Li, Q., X. Li, L. Chen, and D. Wu (2022). Distilling knowledge on text graph for social media attribute inference. In *Proceedings of the 45th International ACM SIGIR Conference on Research and Development in Information Retrieval (SIGIR)*, pp. 2024–2028. ACM.

Liu, M., E. Katsevich, L. Janson, and A. Ramdas (2022). Fast and powerful conditional randomization testing via distillation. *Biometrika* 109(2), 277–293.

Loader, C. R. (1996). Change point estimation using nonparametric regression. *The Annals of Statistics* 24(4), 1667–1678.

Menec, V. H., C. Black, L. MacWilliam, and F. Y. Aoki (2003, Jan–Feb). The impact of influenza-associated respiratory illnesses on hospitalizations, physician visits, emergency room visits, and mortality. *Canadian Journal of Public Health* 94(1), 59–63.

Müller, H.-G. (1992). Change-points in nonparametric regression analysis. *The Annals of Statistics* 20(2), 737–761.

Nie, L. and D. Nicolae (2022). Detection and localization of changes in conditional distributions. *Advances in Neural Information Processing Systems* 35, 36216–36229.

Ploberger, W. and W. Krämer (1992). The cusum test with ols residuals. *Econometrica* 60(2), 271–285.

Rinaldo, A., D. Wang, Q. Wen, R. Willett, and Y. Yu (2021). Localizing changes in high-dimensional regression models. In *International Conference on Artificial Intelligence and Statistics*, pp. 2089–2097. PMLR.

Robbins, M. W., C. M. Gallagher, and R. B. Lund (2016). A general regression changepoint test for time series data. *Journal of the American Statistical Association* 111(514), 670–683.

Su, L. and H. White (2010). Testing structural change in partially linear models. *Econometric Theory* 26(6), 1761–1806.

Su, L. and Z. Xiao (2008). Testing structural change in time-series nonparametric regression models. *Statistics and its Interface* 1(2), 347.

Tansey, W., V. Veitch, H. Zhang, R. Rabadian, and D. M. Blei (2022). The holdout randomization test for feature selection in black box models. *Journal of Computational and Graphical Statistics* 31(1), 151–162.

Vogt, M. (2015). Testing for structural change in time-varying nonparametric regression models. *Econometric Theory* 31(4), 811–859.

Wang, D., Z. Zhao, K. Z. Lin, and R. Willett (2021). Statistically and computationally efficient change point localization in regression settings. *Journal of Machine Learning Research* 22(248), 1–46.

A EM Algorithm for MEND-LAD

In this section, we detail the use of the Expectation-Maximization (EM) algorithm to estimate the conditional distributions $p_0(Y | \mathbf{X})$ and $p_1(Y | \mathbf{X})$ in MEND-LAD. The EM algorithm is utilized to fit a mixture model to the data, capturing the relationship between Y and \mathbf{X} under the pre- and post-change regimes.

A.1 Latent Variable Model

We introduce a latent binary variable Z to indicate the regime of each observation:

$$Z_i = \begin{cases} 0, & \text{if } R_i \leq \tau, \\ 1, & \text{if } R_i > \tau, \end{cases}$$

where $Z_i = 0$ corresponds to the pre-change regime and $Z_i = 1$ corresponds to the post-change regime. The conditional distribution of Y given \mathbf{X} and Z is expressed as:

$$p(Y | \mathbf{X}, Z) = \begin{cases} p_0(Y | \mathbf{X}), & \text{if } Z = 0, \\ p_1(Y | \mathbf{X}), & \text{if } Z = 1. \end{cases}$$

The mixing proportions $\pi_0(\mathbf{X})$ and $\pi_1(\mathbf{X})$ are functions of \mathbf{X} , reflecting the dependence of the regime probabilities on the covariates \mathbf{X} . The goal of the EM algorithm is to estimate the parameters of $p_0(Y | \mathbf{X})$, $p_1(Y | \mathbf{X})$, as well as $\pi_0(\mathbf{X})$ and $\pi_1(\mathbf{X})$, by maximizing the observed data log-likelihood:

$$\log p(Y, \mathbf{X}) = \sum_{i=1}^n \log [\pi_0(\mathbf{X}_i)p_0(Y_i | \mathbf{X}_i) + \pi_1(\mathbf{X}_i)p_1(Y_i | \mathbf{X}_i)].$$

A.2 EM Algorithm Steps

The EM algorithm alternates between the following steps until convergence:

- **E-step:** Compute the posterior probabilities of the latent variable Z for each observation i , given the current estimates of $p_0(Y | \mathbf{X})$, $p_1(Y | \mathbf{X})$, $\pi_0(\mathbf{X})$, and $\pi_1(\mathbf{X})$:

$$\Pr(Z_i = 0 | Y_i, \mathbf{X}_i) = \frac{p_0(Y_i | \mathbf{X}_i)\pi_0(\mathbf{X}_i)}{p_0(Y_i | \mathbf{X}_i)\pi_0(\mathbf{X}_i) + p_1(Y_i | \mathbf{X}_i)\pi_1(\mathbf{X}_i)},$$

$$\Pr(Z_i = 1 | Y_i, \mathbf{X}_i) = \frac{p_1(Y_i | \mathbf{X}_i)\pi_1(\mathbf{X}_i)}{p_0(Y_i | \mathbf{X}_i)\pi_0(\mathbf{X}_i) + p_1(Y_i | \mathbf{X}_i)\pi_1(\mathbf{X}_i)}.$$

- **M-step:** Update the parameters of $p_0(Y | \mathbf{X})$, $p_1(Y | \mathbf{X})$, $\pi_0(\mathbf{X})$, and $\pi_1(\mathbf{X})$ by maximizing the expected log-likelihood of the data, weighted by the posterior probabilities computed in the E-step. Specifically:

$$\pi_0(\mathbf{X}) = \frac{\sum_{i=1}^n \Pr(Z_i = 0 | Y_i, \mathbf{X}_i)}{n}, \quad \pi_1(\mathbf{X}) = \frac{\sum_{i=1}^n \Pr(Z_i = 1 | Y_i, \mathbf{X}_i)}{n}.$$

The parameters of $p_0(Y | \mathbf{X})$ and $p_1(Y | \mathbf{X})$ are updated using weighted regression or other appropriate methods, depending on the model assumptions for p_0 and p_1 .

A.3 Output

The EM algorithm outputs the distilled representation $d(\mathbf{X})$, which includes the following components:

- $\hat{m}_0(\mathbf{X})$ and $\hat{m}_1(\mathbf{X})$: The estimated conditional means for Y in the pre-change and post-change regimes, respectively.
- $\hat{\beta}_0$ and $\hat{\beta}_1$: The estimated coefficients of the regression models for $p_0(Y | \mathbf{X})$ and $p_1(Y | \mathbf{X})$, respectively (if applicable).
- $\hat{\pi}_0(\mathbf{X})$ and $\hat{\pi}_1(\mathbf{X})$: The estimated mixing proportions as functions of \mathbf{X} .

These distilled components $d(\mathbf{X})$ are subsequently used in MEND-LAD to efficiently compute the test statistic and detect change points.

B Proofs

Proposition B.1. Assume we have sequential data $\mathcal{D} = \{(Y_i, \mathbf{X}_i, R_i)\}_{i=1}^n$. Given R_i with each observation (Y_i, \mathbf{X}_i) follows the generative model:

$$Y, \mathbf{X} \mid R \sim p_{\mathbf{X}|R}(\mathbf{X})p_{Y|\mathbf{X}}(Y), \quad (7)$$

Now define $\mathcal{D}^* = \{(Y_i, \mathbf{X}_i, R_i^*)\}_{i=1}^n$, where each $R_i^* \sim p_{R|\mathbf{X}_i}(t)$, then any test statistic $S(\mathcal{D})$ obeys:

$$S(\mathcal{D}^*)|(Y, \mathbf{X}) \stackrel{d}{=} S(\mathcal{D})|(Y, \mathbf{X}) \quad (8)$$

Proof of Proposition B.1. Under the model, given R , the covariates \mathbf{X} are generated first from $p_{\mathbf{X}|R}(\mathbf{X})$, and then the response Y is generated from $p_{Y|\mathbf{X}}(Y)$ independently of R . This implies the conditional independence:

$$Y \perp R \mid \mathbf{X}. \quad (9)$$

To prove the claim, it suffices to show that R and R^* have the same distribution conditionally on (Y, \mathbf{X}) . This follows from

$$R^* \mid (Y, \mathbf{X}) \stackrel{d}{=} R \mid X \stackrel{d}{=} R \mid (Y, \mathbf{X}).$$

The first equality comes from the definition of R^* while the second follows from the conditional independence of Y and R , and therefore any statistic computed from (Y, \mathbf{X}, R) has the same distribution as one computed from (Y, \mathbf{X}, R^*) , conditionally on (Y, \mathbf{X}) . \square

B.1 Proof of Theorem 2.1

Assume the null hypothesis

$$H_0 : p_{Y|\mathbf{X}, R}(y) = p_{Y|\mathbf{X}}(y), \quad \text{for all } R \in \{1, \dots, T\},$$

holds. If we use the test statistic $S(\mathcal{D})$ and the resampled data sets $\mathcal{D}^{(k)}$ defined in Algorithm 1, then by Proposition B.1, we have:

$$S(\mathcal{D}^{(k)}) \mid (Y, \mathbf{X}) \stackrel{d}{=} S(\mathcal{D}) \mid (Y, \mathbf{X}), \quad \text{for all } k = 1, \dots, K. \quad (10)$$

Therefore, the p -value is defined as

$$\text{p-value} = \frac{1}{K+1} \left(1 + \sum_{k=1}^K \mathbb{I}(S(\mathcal{D}^{(k)}) \geq S(\mathcal{D})) \right)$$

is valid under H_0 . Specifically,

$$\mathbb{P}(\text{p-value} \leq \alpha) = \mathbb{P} \left(S(\mathcal{D}^{(k)}) > S(\mathcal{D}) \text{ for less than } \alpha(K+1) \text{ values of } k \right) \leq \alpha.$$

Hence, under H_0 ,

$$\lim_{n \rightarrow \infty} \mathbb{P}(\text{Algorithm 1 rejects}) \leq \alpha.$$

C Additional Details on Numerical Studies

C.1 Additional Details of Simulation

In this appendix, we provide the detailed implementation procedures in the numerical studies. In the MEND model, we adopt the Lasso estimator for (3), and in both the MEND and MEND-LAD models, we estimate the distribution $p(R \mid \mathbf{X})$ using logistic regression as described in Section 2.4. Unlike the proposed methods, the benchmark approaches are originally developed for settings where only one sample is observed at each time point. However, in our setting, multiple samples are available at each time point. To enable a fair comparison and adapt these methods to our setting, we concatenate the data sequentially over time as described in the previous section, treating the combined dataset as a single sequence for change-point analysis. For each benchmark method, we

adopt the default settings recommended in the corresponding papers or software packages unless otherwise specified.

Following [Nie and Nicolae \(2022\)](#), the p -values in KCE and KCD is determined by 500 bootstraps. Since KCE and KCD are not directly applicable in high-dimensional settings, we perform variable screening using the SCAD penalty ([Fan and Li, 2001](#)) before applying these methods to ensure efficient and accurate analysis in the high-dimensional setting. For the kernel bandwidth h , it is tuned among $S_h = \{0.001, 0.1, 0.2, 0.3, 0.4, 0.5, 1, 3, 5, 10, 15\}$, which is similar to that of [Nie and Nicolae \(2022\)](#). For each scenario, the selected bandwidths h for KCD and KCE are as follows.

Table 5: The selected bandwidth h for KCD and KCE

h	Scenario 1	Scenario 2	Scenario 3
h-KCD	0.4	0.5	0.5
h-KCE	0.2	0.2	0.1

C.2 Details on Pseudo-simulation

For the pseudo simulation, the covariates \mathbf{X}_i are taken from the real data. We assume there is no change point, meaning that the data across all months follow the same underlying model. Pseudo outcomes are generated from a binomial distribution:

$$Y_{\text{pseudo},i} \sim \text{Binomial} \left(\frac{\exp(\hat{\eta}^T \mathbf{X}_i)}{1 + \exp(\hat{\eta}^T \mathbf{X}_i)} \right)$$

where $\hat{\eta}$ is a fixed coefficient vector applied uniformly across all months. The Type-I error rate is estimated by calculating the p -values for each method using \mathbf{X}_i and $Y_{\text{pseudo},i}$, and repeating this process 500 times.